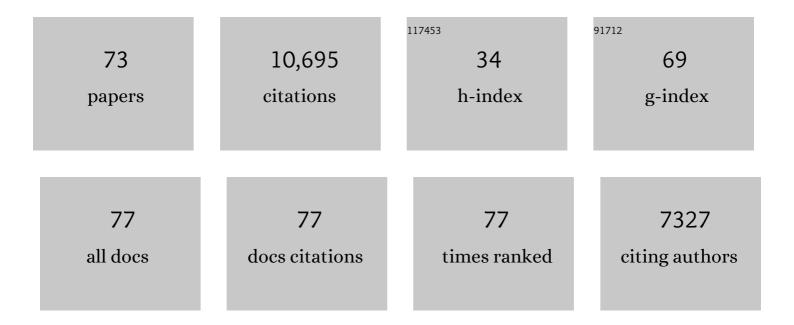
List of Publications by Year in descending order

Source: https://exaly.com/author-pdf/5756517/publications.pdf Version: 2024-02-01



ALLISON REESE

#	Article	IF	CITATIONS
1	Additive manufacturing of metallic components – Process, structure and properties. Progress in Materials Science, 2018, 92, 112-224.	16.0	4,751
2	Anisotropic tensile behavior of Ti–6Al–4V components fabricated with directed energy deposition additive manufacturing. Acta Materialia, 2015, 87, 309-320.	3.8	1,044
3	Materials for additive manufacturing. CIRP Annals - Manufacturing Technology, 2017, 66, 659-681.	1.7	684
4	Effect of processing parameters on microstructure and tensile properties of austenitic stainless steel 304L made by directed energy deposition additive manufacturing. Acta Materialia, 2016, 110, 226-235.	3.8	577
5	Functionally graded material of 304L stainless steel and inconel 625 fabricated by directed energy deposition: Characterization and thermodynamic modeling. Acta Materialia, 2016, 108, 46-54.	3.8	432
6	Additive manufacturing of a functionally graded material from Ti-6Al-4V to Invar: Experimental characterization and thermodynamic calculations. Acta Materialia, 2017, 127, 133-142.	3.8	298
7	Residual stress mapping in Inconel 625 fabricated through additive manufacturing: Method for neutron diffraction measurements to validate thermomechanical model predictions. Materials and Design, 2017, 113, 169-177.	3.3	247
8	Review of Mechanical Properties of Ti-6Al-4V Made by Laser-Based Additive Manufacturing Using Powder Feedstock. Jom, 2016, 68, 724-734.	0.9	217
9	Partially coupled anisotropic fracture model for aluminum sheets. Engineering Fracture Mechanics, 2010, 77, 1128-1152.	2.0	184
10	Advances in additive manufacturing of metal-based functionally graded materials. International Materials Reviews, 2021, 66, 1-29.	9.4	169
11	Effect of stress triaxiality and Lode angle on the kinetics of strain-induced austenite-to-martensite transformation. Acta Materialia, 2011, 59, 2589-2600.	3.8	148
12	Effect of processing conditions on the microstructure, porosity, and mechanical properties of Ti-6Al-4V repair fabricated by directed energy deposition. Journal of Materials Processing Technology, 2019, 264, 172-181.	3.1	111
13	Bio-Inspired Carbon Nanotube–Polymer Composite Yarns with Hydrogen Bond-Mediated Lateral Interactions. ACS Nano, 2013, 7, 3434-3446.	7.3	103
14	Crystallographic texture in an additively manufactured nickel-base superalloy. Materials Science & Engineering A: Structural Materials: Properties, Microstructure and Processing, 2017, 684, 47-53.	2.6	89
15	Characterization of a functionally graded material of Ti-6Al-4V to 304L stainless steel with an intermediate V section. Journal of Alloys and Compounds, 2018, 742, 1031-1036.	2.8	89
16	Diffraction and single-crystal elastic constants of Inconel 625 at room and elevated temperatures determined by neutron diffraction. Materials Science & Engineering A: Structural Materials: Properties, Microstructure and Processing, 2016, 674, 406-412.	2.6	86
17	Extraordinary Improvement of the Graphitic Structure of Continuous Carbon Nanofibers Templated with Double Wall Carbon Nanotubes. ACS Nano, 2013, 7, 126-142.	7.3	84
18	Quantitative relationship between anisotropic strain to failure and grain morphology in additively manufactured Ti-6Al-4V. Materials Science & Engineering A: Structural Materials: Properties, Microstructure and Processing, 2017, 706, 287-294.	2.6	78

#	Article	IF	CITATIONS
19	The desmoplakin–intermediate filament linkage regulates cell mechanics. Molecular Biology of the Cell, 2017, 28, 3156-3164.	0.9	70
20	Key Factors Limiting Carbon Nanotube Yarn Strength: Exploring Processing-Structure-Property Relationships. ACS Nano, 2014, 8, 11454-11466.	7.3	68
21	Absence of dynamic strain aging in an additively manufactured nickel-base superalloy. Nature Communications, 2018, 9, 2083.	5.8	59
22	Effect of directed energy deposition processing parameters on laser deposited Inconel® 718: External morphology. Journal of Laser Applications, 2017, 29, .	0.8	56
23	In situ transmission electron microscope tensile testing reveals structure–property relationships in carbon nanofibers. Carbon, 2013, 60, 246-253.	5.4	55
24	Identification of the Direction-Dependency of the Martensitic Transformation in Stainless Steel Using In Situ Magnetic Permeability Measurements. Experimental Mechanics, 2011, 51, 667-676.	1.1	54
25	Effect of chemistry on martensitic phase transformation kinetics and resulting properties of additively manufactured stainless steel. Acta Materialia, 2017, 131, 410-422.	3.8	51
26	Characterization of the Effects of Internal Pores on Tensile Properties of Additively Manufactured Austenitic Stainless Steel 316L. Experimental Mechanics, 2019, 59, 793-804.	1.1	51
27	Characterization of the strength of support structures used in powder bed fusion additive manufacturing of Ti-6Al-4V. Additive Manufacturing, 2017, 14, 60-68.	1.7	49
28	Effect of directed energy deposition processing parameters on laser deposited Inconel® 718: Microstructure, fusion zone morphology, and hardness. Journal of Laser Applications, 2017, 29, .	0.8	48
29	Effect of Substrate Thickness and Preheating on the Distortion of Laser Deposited Ti–6Al–4V. Journal of Manufacturing Science and Engineering, Transactions of the ASME, 2018, 140, .	1.3	47
30	Anisotropic plasticity model coupled with Lode angle dependent strain-induced transformation kinetics law. Journal of the Mechanics and Physics of Solids, 2012, 60, 1922-1940.	2.3	41
31	Stress relaxation behavior and mechanisms in Ti-6Al-4V determined via in situ neutron diffraction: Application to additive manufacturing. Materials Science & Engineering A: Structural Materials: Properties, Microstructure and Processing, 2017, 707, 585-592.	2.6	40
32	Impact of Interlayer Dwell Time on Microstructure and Mechanical Properties of Nickel and Titanium Alloys. Metallurgical and Materials Transactions A: Physical Metallurgy and Materials Science, 2017, 48, 4411-4422.	1.1	39
33	In Situ Scanning Electron Microscope Peeling To Quantify Surface Energy between Multiwalled Carbon Nanotubes and Graphene. ACS Nano, 2014, 8, 124-138.	7.3	37
34	Experimental validation of Scheil–Gulliver simulations for gradient path planning in additively manufactured functionally graded materials. Materialia, 2020, 11, 100689.	1.3	36
35	Stress relaxation in a nickel-base superalloy at elevated temperatures with in situ neutron diffraction characterization: Application to additive manufacturing. Materials Science & Engineering A: Structural Materials: Properties, Microstructure and Processing, 2018, 714, 75-83.	2.6	35
36	Cold Sintering Na <sub>2</sub> Mo <sub>2</sub> O <sub>7</sub> Ceramic with Poly(ether imide) (PEI) Polymer to Realize High-Performance Composites and Integrated Multilayer Circuits. ACS Applied Nano Materials, 2018, 1, 3837-3844.	2.4	35

#	Article	IF	CITATIONS
37	Multiaxial plasticity and fracture behavior of stainless steel 316L by laser powder bed fusion: Experiments and computational modeling. Acta Materialia, 2020, 199, 578-592.	3.8	35
38	Defectâ€Tolerant Nanocomposites through Bioâ€Inspired Stiffness Modulation. Advanced Functional Materials, 2014, 24, 2883-2891.	7.8	28
39	Anisotropic multiaxial plasticity model for laser powder bed fusion additively manufactured Ti-6Al-4V. Materials Science & Engineering A: Structural Materials: Properties, Microstructure and Processing, 2018, 738, 90-97.	2.6	28
40	Analysis of formation and growth of the $\ddot{\rm l}f$ phase in additively manufactured functionally graded materials. Journal of Alloys and Compounds, 2020, 814, 151729.	2.8	28
41	Fracture of laser powder bed fusion additively manufactured Ti–6Al–4V under multiaxial loading: Calibration and comparison of fracture models. Materials Science & Engineering A: Structural Materials: Properties, Microstructure and Processing, 2019, 761, 137967.	2.6	21
42	Experimental analysis and thermodynamic calculations of an additively manufactured functionally graded material of V to Invar 36. Journal of Materials Research, 2018, 33, 1642-1649.	1.2	20
43	Stress state-dependent mechanics of additively manufactured 304L stainless steel: Part 1 – characterization and modeling of the effect of stress state and texture on microstructural evolution. Materials Science & amp; Engineering A: Structural Materials: Properties, Microstructure and Processing, 2019, 743, 811-823.	2.6	20
44	Impact of retained austenite on the aging response of additively manufactured 17-4ÂPH grade stainless steel. Materials Science & Engineering A: Structural Materials: Properties, Microstructure and Processing, 2021, 817, 141363.	2.6	20
45	Plasticity and fracture behavior of Inconel 625 manufactured by laser powder bed fusion: Comparison between as-built and stress relieved conditions. Materials Science & Engineering A: Structural Materials: Properties, Microstructure and Processing, 2021, 806, 140808.	2.6	19
46	xmlns:mml="http://www.w3.org/1998/Math/MathML"> <mml:mrow> <mml:mi mathvariant="normal"&gt;N <mml:msub> <mml:mi mathvariant="normal"&gt;i <mml:mn>3</mml:mn> </mml:mi </mml:msub> <mml:mi>Al</mml:mi> </mml:mi </mml:mrow> from stacking fault energy and ideal strength: A first-principles study via pure alias shear	mi:math>	18
47	deformation. Physical Review B, 2020, 101, . DFTTK: Density Functional Theory ToolKit for high-throughput lattice dynamics calculations. Calphad: Computer Coupling of Phase Diagrams and Thermochemistry, 2021, 75, 102355.	0.7	17
48	Contrasting the Role of Pores on the Stress State Dependent Fracture Behavior of Additively Manufactured Low and High Ductility Metals. Materials, 2021, 14, 3657.	1.3	15
49	Micromechanics of multiaxial plasticity of DP600: Experiments and microstructural deformation modeling. Materials Science & amp; Engineering A: Structural Materials: Properties, Microstructure and Processing, 2018, 721, 168-178.	2.6	14
50	Tensile behavior of stainless steel 304L to Ni-20Cr functionally graded material: Experimental characterization and computational simulations. Materialia, 2021, 18, 101151.	1.3	14
51	In situ electron microscopy tensile testing of constrained carbon nanofibers. International Journal of Mechanical Sciences, 2018, 149, 452-458.	3.6	13
52	Correlation analysis of materials properties by machine learning: illustrated with stacking fault energy from first-principles calculations in dilute fcc-based alloys. Journal of Physics Condensed Matter, 2021, 33, 295702.	0.7	13
53	Stress state-dependent mechanics of additively manufactured 304L stainless steel: Part 2 – Characterization and modeling of macroscopic plasticity behavior. Materials Science & Engineering A: Structural Materials: Properties, Microstructure and Processing, 2019, 743, 824-831.	2.6	12
54	Multiaxial fracture of DP600: Experiments and finite element modeling. Materials Science & Engineering A: Structural Materials: Properties, Microstructure and Processing, 2020, 785, 139386.	2.6	11

#	Article	IF	CITATIONS
55	Combined effects of porosity and stress state on the failure behavior of laser powder bed fusion stainless steel 316L. Additive Manufacturing, 2021, 39, 101862.	1.7	10
56	Influence of phase and interface properties on the stress state dependent fracture initiation behavior in DP steels through computational modeling. Materials Science & Engineering A: Structural Materials: Properties, Microstructure and Processing, 2020, 776, 138981.	2.6	9
57	Effect of stress triaxiality and penny-shaped pores on tensile properties of laser powder bed fusion Ti-6Al-4V. Additive Manufacturing, 2021, 48, 102414.	1.7	8
58	Use of ultrasound to identify microstructure-property relationships in 316 stainless steel fabricated with binder jet additive manufacturing. Additive Manufacturing, 2022, 51, 102591.	1.7	8
59	Effect of processing parameters on pore structures, grain features, and mechanical properties in Ti-6Al-4V by laser powder bed fusion. Additive Manufacturing, 2022, 56, 102915.	1.7	8
60	Design of an additively manufactured functionally graded material of 316 stainless steel and Ti-6Al-4V with Ni-20Cr, Cr, and V intermediate compositions. Additive Manufacturing, 2022, 51, 102649.	1.7	7
61	Microstructure and Mechanical Properties of AM Builds. , 2018, , 81-92.		6
62	Effect of processing parameters and strut dimensions on the microstructures and hardness of stainless steel 316L lattice-emulating structures made by powder bed fusion. Additive Manufacturing, 2021, 40, 101943.	1.7	6
63	Full Field Strain Measurement of Material Extrusion Additive Manufacturing Parts with Solid and Sparse Infill Geometries. Jom, 2019, 71, 871-879.	0.9	5
64	Identification of stress state dependent fracture micromechanisms in DP600 through representative volume element modeling. International Journal of Mechanical Sciences, 2021, 194, 106209.	3.6	5
65	Ultrasonic Characterization of Porosity in Components Made by Binder Jet Additive Manufacturing. Materials Evaluation, 2022, 80, 37-44.	0.1	4
66	Orientation and stress state dependent plasticity and damage initiation behavior of stainless steel 304L manufactured by laser powder bed fusion additive manufacturing. Extreme Mechanics Letters, 2021, 45, 101271.	2.0	3
67	Isotropic Phase Transformation in Anisotropic Stainless Steel 301LN Sheets. , 2009, , .		3
68	Predictive Crystal Plasticity Modeling of Single Crystal Nickel Based on First-Principles Calculations. Jom, 2022, 74, 1423-1434.	0.9	2
69	Insight into ideal shear strength of Ni-based dilute alloys using first-principles calculations and correlational analysis. Computational Materials Science, 2022, 212, 111564.	1.4	1
70	Experimental Characterization of Microstructure Evolution in Austenitic Stainless Steel With Phase Transformation. , 2008, , .		0
71	In Situ Transmission Electron Microscopy: Mechanical Testing. , 2015, , 1-12.		0
72	. Finite Element Analysis on Stellite 17mm Tube Valve for Pediatric Ventricular Assist Device. , 2017, , .		0

#	Article	IF	CITATIONS
73	Analysis of Formation and Growth of the $\hat{\Gamma}$ Phase in Additively Manufactured Functionally Graded Materials. SSRN Electronic Journal, 0, , .	0.4	Ο